

Highly Efficient Abiotic Assay Formats for Methyl Parathion – MINA as Alternative to ELISA

Cem Esen,^{†,‡} Joanna Czulak,^{*,§} Todd Cowen,[‡] Elena Piletska,[‡] and Sergey A. Piletsky[‡]

[†] Department of Chemistry, Faculty of Arts and Sciences, Aydın Adnan Menderes University, 09010 Aydın, Turkey

[‡] Department of Chemistry, University of Leicester, LE1 7RH Leicester, UK

[§] MIP Diagnostics Ltd, Colworth Park, MK44 1LQ Bedford, UK

ABSTRACT: Enzyme-linked immunosorbent assay (ELISA) is a widely used standard method for sensitive detection of analytes of environmental, clinical or biotechnological interest. However, ELISA has clear drawbacks related to the use of relatively unstable antibodies and enzyme conjugates, and need in several steps such as washing of non-bound conjugates and adding dye reagents. Herein we introduce a new completely abiotic assay where antibodies and enzymes are replaced with fluorescent molecularly imprinted polymer nanoparticles (nanoMIPs) and target-conjugated magnetic nanoparticles, which acted as both reporter probes and binding agents. The components of the molecularly imprinted polymer nanoparticles assay (MINA) are assembled in microtiter plates fitted with magnetic inserts. We have compared performance of new magnetic assay with MIP-based ELISA for the detection of methyl parathion (MP). Both assays have shown high sensitivity toward allowing detection of MP at picomolar concentrations without any cross-reactivity against chlorpyrifos and fenthion. The fully abiotic assays were also proven to detect analyte in real samples such as tap water and milk. Unlike ELISA-based systems the novel assay required no washing steps or addition of enzyme substrates, making it more user-friendly and suitable for high throughput screening.

Methyl Parathion (MP) is an organophosphorus insecticide and acaricide that is toxic to several organs, acting on central nervous system by inhibiting acetylcholinesterase.^{1,2} This effect can lead to neuronal disorder, organ failure and even death.³ The public concern over MP has increased in recent times due to reports of its adverse genotoxic effects on somatic and sperm cells.⁴⁻⁷ Although, MP has been banned for application in agricultural fields due to its high toxicity, its misuse continues in many countries. Accordingly to the World Health Organization (WHO) guidelines for drinking water quality, the Methyl Parathion concentration in natural agricultural waters ranges up to 0.46 $\mu\text{g L}^{-1}$ increasing during summer months.⁸ The regulations of Environmental Protection Agency (EPA) suggest that safe levels of methyl parathion in drinking water that will not cause harm to health are following: 0.3 mg L^{-1} (1.1 μM) for 1 or 10 days of exposure for children, 0.03 mg L^{-1} (0.11 μM) for longer term exposure for children, and 0.002 mg L^{-1} (7.6 nM) for life-time exposure of adults.⁹ Highly sensitive detection of MP is therefore of great importance in real-world samples to ensure food and environment safety.

Several analytical techniques have been developed for sensitive and selective determination of MP, such as gas chromatography,¹⁰ liquid/gas chromatography-mass spectrometry,¹¹⁻¹³ electrochemical methods,¹⁴⁻¹⁶ immunoassay,¹⁷ surface-enhanced Raman spectroscopy,¹⁸ fluorescence,¹⁹ and chemiluminescence.²⁰ Nevertheless, expensive instrumentation, complicated and tedious sample preparation, pre-concentration, cleaning and often derivatization become driving forces to investigate new, simple and inexpensive methods for the determination of MP.

Herein we present a new highly efficient analytical method that can be applied for quantitative analysis of MP samples in the form of an abiotic assay that relies on use of molecularly imprinted polymer nanoparticles (MINA).²¹ MINA has been proved as a potential replacement for enzyme-linked immunosorbent assay (ELISA) where molecularly imprinted polymer nanoparticles (nanoMIPs) replace antibodies exhibiting very similar selectivity, affinity and specificity.^{21, 22} However, ELISA requires multiple steps including washing, blocking, and addition of enzyme substrates. That is why there is a need to develop inexpensive, robust and simple assays which do not rely on cold-chain storage, and which can be performed by technicians with no or little training.

Two variants of assays were applied for the detection of the pesticide MP: pseudo-ELISA with nanoMIPs replacing only antibodies and which still relied on use of analyte-enzyme conjugate for signal amplification; and MINA, where nanoMIPs and magnetic nanoparticles with immobilized analyte replaced both, antibodies and enzymes. Another important advantage of MINA is that it doesn't involve any washing steps, which are common for ELISA, and in fact consist of only one liquid-handling step, specifically, addition of the sample. MINA for MR is effective and simple system, which generates quantitative data within an hour.

MATERIALS AND METHODS

Materials. 3-(trimethoxysilyl)propyl methacrylate, *N*-(3-(trimethoxysilyl)propyl)ethylenediamine, glutaraldehyde (GA),

acrylamide (AAm), trimethylolpropane trimethacrylate (TRIM), ethylene glycol dimethacrylate (EGDMA), pentaerythritol tetrakis(3-mercaptopropionate) (PETMP), 2-(morpholino) ethanesulfonic acid (MES), 1-ethyl-3-(3-dimethylaminopropyl)-carbodiimide hydrochloride (EDC), *N*-hydroxysuccinimide (NHS), horseradish peroxidase (HRP), solution of 3,3',5,5'-tetramethylbenzidine (TMB), Tween 20 and iron (II, III) oxide nanopowder (Fe₃O₄) (particle size \leq 50 nm) were purchased from Sigma-Aldrich, UK. Glass beads SPHERIGLASS® A-Glass 2429 (70–100 μ m diameter), were purchased from Potters Industries LLC, UK. Amino parathion (AP) was purchased from Angene International Limited, China. Methyl parathion (MP), Fenthion (F), and Chlorpyrifos (CP) were purchased from Sigma-Aldrich, UK. Ethylene glycol methacrylate phosphate (EGMP) was obtained from BOC Sciences, UK. Phosphate buffered saline (PBS) was prepared as directed from 1 x PBS buffer tablet (Gibco, UK), pH 7.2, at 25 °C. Kolliphor P188 polymer was a gift from BASF, UK. Acetonitrile (ACN), dimethyl sulfoxide (DMSO) and sodium hydroxide (NaOH) were obtained from Fisher Scientific, UK. Bovine Serum Albumin (BSA) was obtained from Acros Organics, UK. *N,N*-diethyldithiocarbamic acid benzyl ester >98 % (iniferter) was obtained from TCI Europe, UK. *N*-fluoresceinylacrylamide was synthesized as previously described and provided by MIP Diagnostic Ltd, UK.²³ Clear bottom 96-well microtiter plates were purchased from Thermo Scientific, UK. Adhesive-backed, 0.5 mm thickness magnetic sheets were purchased from Polarity Magnets, UK. Double-distilled ultrapure water (Millipore, UK) was used for all experiments. Skimmed milk was obtained from a local supermarket. Tap water sample was collected from the laboratory tap. All chemicals and solvents were of analytical or HPLC grade and used without further purification.

Computational modelling. Molecular modelling was performed using the software package SYBYL 7.3 (Tripos Inc. ST. Louis, MO, USA). A molecular mechanics based automated screening technique employing the Leapfrog algorithm present in Sybyl software was used for the selection of monomers with high affinity to both the template (Amino Parathion) and analyte (Methyl Parathion). The structures of both molecules are shown in Figure S1 in SI.

Both compounds were first drawn and energetically minimized with the Tripos force field and applied Gasteiger-Huckel charges. The resulting structure was then screened against a database consisting of 28 commonly used functional monomers (Figure S2 in SI), resulting a table ranking these monomers by their affinity for the molecule. The screening was performed for 60,000 iterations to achieve self-consistency in binding scores, and the results are analyzed for suitability in the chosen reaction conditions.

Immobilization of the template onto the solid phase. Glass beads (GB, 75 μ m) were activated by boiling them with 4 M NaOH for 20 min and washed with deionized water (DI). Afterwards, the GB were placed in sulfuric acid-water (1:1) solution for 30 min and again washed respectively with water, PBS and acetone. After drying the GB were silanized using *N*-(3-(trimethoxysilyl)propyl)ethylenediamine 2 % (v/v, 0.4 mL solution/g of GB) in anhydrous toluene overnight at 70 °C with addition of dipodal silane (1,2-Bis(trimethoxysilyl)ethane) as 330 μ L per 100 mL of toluene; then washed with MeOH, acetone and dried. Afterwards, the beads were incubated for 2 h in a 5 % v/v glutaraldehyde (GA) solution in PBS, pH 7.2 and then

washed with deionized water. The immobilization of the template (amino parathion, AP) was performed by incubation of GA-derivatized GB in a template solution (1 mg mL⁻¹ in MeOH/H₂O) at room temperature (RT), pH 7.2, for 4 hours. During incubation, sodium cyano borohydride (1 mg mL⁻¹) was added into the immobilization mixture. Afterwards, the GB with immobilized template were washed with MeOH and water, then dried under vacuum and stored at 4 °C until further use.

Synthesis of nanoMIPs. NanoMIPs were synthesized using the solid-phase synthesis procedure described previously with minor modifications.²⁴ Two types of nanoMIPs were prepared depending on the final application: fluorescent nanoMIPs (F-nanoMIPs) for magnetic assay and colorless non-fluorescent nanoMIPs (nanoMIPs) for pseudo-ELISA assay. For the synthesis of fluorescent nanoMIPs; AAm (0.48 g), EGMP (5.63 g), TRIM (3.24 g), EGDMA (3.24 g), PETMP (0.2 g) and *N*-fluoresceinylacrylamide (0.1 g) were dissolved in 11 mL of DMSO:ACN (50 % v/v). Then 0.75 g of iniferter *N,N*-diethyldithiocarbamic acid benzyl ester was added to the monomer mixture. Afterwards, 30 g of amino parathion-functionalized GBs were added to the polymerization mixture. Again, the glass beads and polymerization mixture were purged with nitrogen for 5 min. Then polymerization reaction was initiated by UV light and carried out for 1.5 min at RT. Before the collection of the high affinity nanoMIPs, the solid-phase was washed to remove unreacted monomers and low affinity nanoparticles using respectively DMSO (10 mL \times 5) and ACN (25 mL \times 10) at 0 °C. Then high affinity nanoMIPs were collected by using hot ACN (10 mL \times 10 times) at 65 °C. The non-fluorescent nanoMIPs were synthesized in the same manner, but without addition of the fluorescent monomer in the polymerization mixture. Eventually, the solution of high affinity nanoMIPs was concentrated by ultrafiltration on a Millipore Amicon Ultra centrifugal filter unit (10 kDa MWCO) and used in magnetic assays and pseudo-ELISA tests.

Development of pseudo-ELISA assay. The Amino Parathion-horseradish peroxidase (AP-HRP) conjugate was prepared as follows: HRP (10 mg) was dissolved in 10 mL of 0.1 M MES buffer (pH 6.0, 1 mL) to the final concentration of 1 mg mL⁻¹, then 0.4 mg of EDC (0.4 mg) and 1.1 mg of NHS were added. The reaction was allowed to proceed at RT for 15 min. The buffer was then removed by ultrafiltration using Millipore Amicon Ultra centrifugal filter unit with cut-off membrane of 30 kDa. Subsequently, AP (molar ratio of AP to HRP 1:1) was dissolved in 10 mL of DMSO:PBS / (20:80 %) at pH 7.4 and then added to the activated HRP. The reaction was allowed to proceed for another 2 h at 4 °C. After coupling, the conjugate was washed ten times with 5 mL of PBS using Millipore Amicon Ultra centrifugal filter with cut-off membrane of 10 kDa to remove any free Amino Parathion. After washing the conjugate was dissolved in deionized water (2 mL) and stored at -18 °C until further use.

Imprinted polymeric nanoparticles (100 μ L, 0.06 mg mL⁻¹) were dispensed into the wells of a 96-well microtiter plate and left to dry overnight at ambient temperature. Subsequently, each well of the microtiter plate was washed three times using 200 μ L of PBS. After washing, 300 μ L of blocking solution consisting of 0.1% BSA and 1 % of Tween 20 in PBS and incubated for 1 h at RT. After blocking each well of the microtiter plate was washed 3 times using 200 μ L of PBS. The plate was then tapped on the paper towel to remove water, dried and was stored until use.

The concentration of the AP-HRP conjugate was optimized for specific binding by comparing MIP-containing and empty wells. In the blank assay, 100 μL of different conjugate dilutions (from 1:200 to 1:1600) were incubated for 1 h within the wells with and without nanoMIPs. Non-bound conjugate was then removed by washing with three times with 300 μL of blocking solution and then with 300 μL of PBS. Subsequently, 100 μL of TMB was added and incubated for 10 min. Finally, the reaction was stopped using 100 μL of 0.5 M H_2SO_4 . The absorbance (ABS) was measured for each well at a wavelength of 450 nm using UV-vis microtiter plate reader (Dyner, UK). The standard deviations and were obtained for all experiments carried out in triplicates. The optimum concentration of the AP-HRP conjugate was determined as the one which had given the highest difference in color development between the empty wells and wells with nanoMIPs of the microtiter plate. Four hundred times dilution of the AP-HRP stock solution, which was identified as optimum, was used in all subsequent experiments.

The procedure for conducting enzyme-linked assays with nanoMIPs was carried out as described previously.^{25, 26} The surface of the microtiter plate was first blocked using BSA/Tween 20 solution in PBS (0.01%/1%) for 1 h at RT. The microtiter plate was washed three times with 300 μL of PBS. Then, 100 μL of HRP-conjugate/free analyte (i.e. MP) mixture in PBS with final HRP dilution as 1:400 and the final free analyte concentration in a range of 0.1 mM-0.1 nM was added into the wells of microtiter plate and incubated for 1 h at RT. The non-bound HRP-conjugate and free analyte were removed by washing with $3 \times 300 \mu\text{L}$ of BSA/Tween 20 solution in PBS. Finally, 100 μL of TMB was added into the wells and incubated for 10 minutes before the reaction was stopped using 0.5 M H_2SO_4 . The absorbance was measured for each well at a wavelength of 450 nm using the microtiter plate reader. Error bars represent standard deviations and were obtained for all experiments carried out as triplicate. Free analyte (i.e. MP) standard solutions were prepared in PBS buffer, or spiked tap water or milk. Tap water was filtered using 0.2 μm syringe filter before the preparation of sample solutions.

In order to prepare the milk sample skimmed milk was fractionated using centrifugation for 1.5 h at 13,000 rpm (centrifuge Sigma 1-16, SciQuip, UK). After the centrifugation, the middle fraction of the milk sample was collected and fractionated once again under the same conditions. The middle fraction after the second centrifugation was collected and then filtered through 0.2 μm syringe filter, spiked with methyl parathion and used in the assay.

Preparation of microtiter plate with magnetic inserts. The microtiter plate wells were modified with magnetic inserts as previously described.^{27, 28} Inserts with an internal diameter of 3 mm, an external diameter of 6.5 mm and of 0.5 mm thickness were cut from flexible magnetic sheets with self-adhesive backing. These disks were inserted into the bottom of each well of a standard clear flat bottom microtiter plate. In order to reduce the non-specific binding, each well was totally filled with a solution of Kolliphor® P188 (1% w/v) for 10 min, after which the plate was washed well with water and allowed to air dry. Kolliphor® P188 is a surfactant also known as Poloxamer 188 was used here to reduce the non-specific binding and improve the wettability of the polypropylene surfaces of the microtiter plate wells.

Preparation of AP magnetic template (MT). The AP MT was prepared by silanization of 1 g of iron (II, III) oxide nanoparticles (IO-NP) (20-50 nm) using 5 mL of 3-(trimethoxysilyl)propyl methacrylate in 45 mL anhydrous toluene under constant sonication for 4.5 h. Then, the IO-NP were separated from solution using a magnet, washed with toluene and dried. Subsequently the IO-NP were modified using 10 mL of GA solution (7 %, v/v) in PBS for 2 h at RT and were washed with water. The template (AP) was immobilized by incubating IO-NP in 10 mL of MeOH-PBS (7/3, v/v) template solution (1mg mL^{-1}) overnight at RT. Subsequently, the MT was washed respectively with MeOH- H_2O (1:1, v/v) solution and MeOH, before dried under N_2 .

Development of magnetic assay. Parameters including the concentration of magnetic template and concentration of F-nanoMIPs were optimized in order to find the best experimental conditions for the magnetic assay. The first optimization was conducted using two different concentrations of fluorescent nanoMIPs (0.090 and 0.045 mg mL^{-1}) and a wide concentration range of magnetic template (0-20 mg mL^{-1}). 100 μL of different concentrations of magnetic template were then added into the wells of the microtiter plate followed by 100 μL of F-nanoMIPs, before being incubated for 1 h. The fluorescence measurements were performed by a Hidex microtiter plate reader (LabLogic, UK) using an excitation wavelength of 490 nm and an emission wavelength of 520 nm.

100 μL of the magnetic template with the optimized concentration (1 mg mL^{-1}) was added into the wells of the microtiter plate, followed by 50 μL of free MP solution in the range of 4 pM to 0.4 nM. Subsequently, 50 μL of F-nanoMIPs were added into the wells of the microtiter plate and incubated for 1 h (Figure 1). Finally, the fluorescence intensities of supernatants were measured. The application of the magnetic assay for real samples was performed under the same conditions using tap water and milk samples spiked with the same concentrations of MP as stated above.

Physical characterization of nanoMIPs. The concentration of nanoMIPs was calculated from the mass of nanoparticles after evaporation of known volume of the nanoMIPs solution. The size of the nanoparticles was determined by dynamic light scattering (DLS) using a Malvern Zetasizer Nano S instrument (Malvern Instruments, UK) equipped with a 633 nm laser. Three measurements were performed on each sample, each consisting of 6 runs, at 25 °C. The solution of nanoMIPs was sonicated for 5 min before DLS measurement.

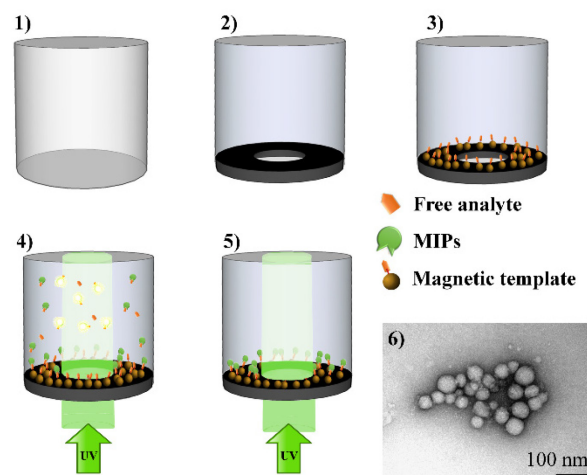


Figure 1. Schematic of MINA assay: 1 – empty non-modified wells, 2 – well with magnetic insert, 3 – well with magnetic template attached to magnetic inserts, 4 – competitive assay in the presence of free analyte and fluorescent MIPs, and 5 – in the absence of analyte, 6 – TEM picture of MIPs.

For TEM visualization, a sample of 3 μL of nanoMIPs was deposited on a carbon-coated grid and allowed to settle for approximately 2 min. Excess of liquid was blotted with tissue paper and then a drop of uranyl acetate stain (1 % v/v aqueous) was deposited and blotted dry with tissue paper. The excess of staining agent was washed out with demineralized water. Visualization was conducted on a JEOL 1400 transmission electron microscope (JEOL, USA) with an accelerating voltage of 80 kV.

RESULTS AND DISCUSSION

Characterization of nanoMIPs. Development of assays based on molecularly imprinted polymers (MIPs) offers potential for a new era of selective and sensitive analyte detection. MIPs are cross-linked synthetic materials synthesized in the presence of a template molecule which serves as a mold for the formation of template-complementary binding sites.²⁹⁻³¹ The resultant polymeric matrix recognizes the template via the imprinted cavity obtained after removal of the template, being complementary to its structure in terms of size, shape and functionality. MIPs can be prepared for a wide variety of targets and are known for their robustness and resistance to variation in pH, solvents, temperature and pressure.³²⁻³⁴ Moreover, owing to superior recognition capabilities, nano-sized MIPs have been developed as antibody mimics for diagnostic and therapeutic applications, for example as drug delivery systems and sensing elements in assays or sensors.^{26, 35-37} In order to obtain the nanoMIPs with cavity complementary to the analyte MP, the analogue AP was used due to the presence of a primary amine which allows the immobilization on both GB and IO-NP.

The molecular modelling was performed for both the template/analogue and the analyte. Two monomers were chosen according to their binding energies and binding position: EGMP and AAm (Figure S3 in SI). The binding energies for both analogue and the template were in a very similar range as shown in

Table 1, and both monomers were used to synthesize MIP nanoparticles.

Table 1. Binding energies between methyl parathion (MP), aminoparathion (AP) and selected monomers.

Monomer	Binding energy for MP	Binding energy for AP
AAm	-27.28	-23.72
EGMP	-24.45	-25.66

The nanoMIPs specific for MP were synthesized as described in the Materials and Methods section. The hydrodynamic diameter of nanoMIPs was measured by DLS and showed a population of nanoparticles with average diameter of 200 nm and a polydispersity index (PdI) of 0.33 for both F-nanoMIPs and colorless nanoMIPs. From TEM images it could be concluded that the size of the dry nanoparticles was in the range of 40–60 nm. The higher diameter values obtained by DLS measurements could be attributed to the swelling of the low cross-linked nanoMIPs in water, which would be expected with this type of polymer.

Performance of pseudo-ELISA assay. An AP-HRP conjugate is required for the enzyme-linked assay. Optimization was carried out using two blocking solutions: 0.1% BSA/1 % Tween 20 and 0.5 % Kolliphor® P188 prepared in PBS buffer. The AP-HRP conjugate concentration was in a range from 1:100 to 1:3200. The results show (Figure S4 in SI) that optimal conjugate dilution was 1:400 due to the highest difference between specific and non-specific binding (an increase of 150 %) when BSA/Tween solution in PBS was used as a blocking agent. Conjugate concentrations that were too high caused an increase in non-specific binding to the empty wells, hence decrease in $\text{ABS}_{\text{MIPs}}/\text{ABS}_{\text{empty}}$. This conjugate concentration was used for all further tests.

The nanoMIPs imprinted for AP were then tested using competitive binding in the pseudo-ELISA assay. The linear response for MP was achieved within the concentration range 0.2 pM to 2.3 pM (Figure 2). No cross-reactivity was detected for pesticides with similar structure such as Chlorpyrifos and Fenthion.

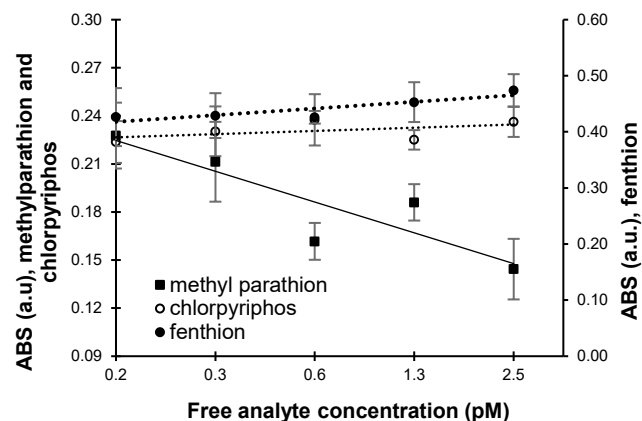


Figure 2. Competitive binding and cross-reactivity using nanoMIPs in pseudo-ELISA.

Optimization of MINA. Firstly, the amount of the magnetic template per well was optimized in order to achieve an efficient binding with F-nanoMIPs. For this aim, experiments were conducted using different concentrations of AP MT in the range of $0.32 \mu\text{g mL}^{-1}$ - 20 mg mL^{-1} and F-nanoMIPs at two different concentrations. The results were obtained as shown in Figure 3.

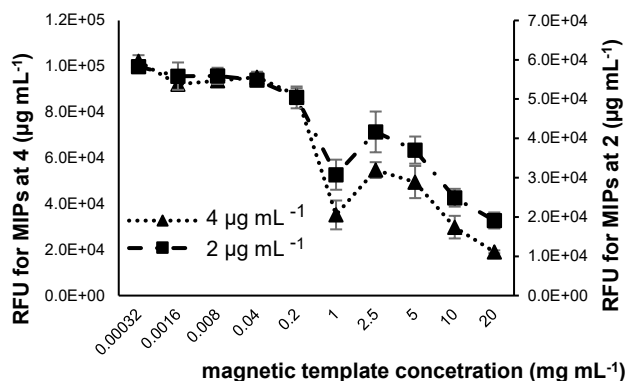


Figure 3. Optimization of magnetic template concentration used for the competitive binding.

Two concentrations of F-nanoMIPs ($2 \mu\text{g mL}^{-1}$ and $4 \mu\text{g mL}^{-1}$) were used to optimize the concentration of MT. In both cases the decrease of fluorescence due to the binding of the F-nanoMIPs to the MT was observed until the concentration of MT reached 1 mg mL^{-1} (Figure 3). A quenching of fluorescence, which was observed at higher concentrations of MT, could be explained by presence of the excess of magnetic material in the central aperture of the inserts, which caused some partial obstruction of light. For all future experiments the lower concentration of F-nanoMIPs ($2 \mu\text{g mL}^{-1}$) and 1 mg mL^{-1} concentration of MT were used.

In order to reduce the non-specific binding microtitre plate was treated with 1% aqueous solution of Kolliphor® P188. After treatment the surface of microtitre plate appeared more hydrophilic as it is appeared that the surfactant was masking hydrophobic interactions. It has indeed resulted in the lower non-specific binding and smaller the standard deviations of the assay by providing easier wettability of the polypropylene wells equipped with magnetic inserts.

Performance of magnetic assay in competitive binding and cross-reactivity. The competitive and cross-reactivity assays were performed in the kinetics mode, measuring the fluorescence in each well every 10 min. The cross-reactivity test was conducted using two very similar compounds, CP and F at the same concentration range as for actual analyte, MP.

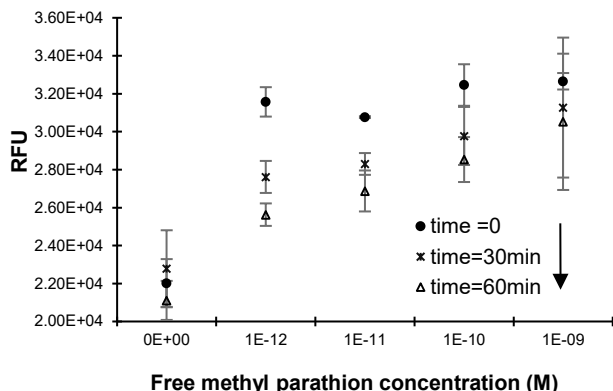


Figure 4. Competitive binding in the magnetic assay for MP at time 0, 30 min and 1 h in DI water.

The results show linear response in the range of $1 \cdot 10^{-12}$ - $1 \cdot 10^{-9}$ M (1 pM - 1 nM) for MP after 1 h of incubation. At time = 0 there is no obvious differences in the fluorescence intensity for the wells with different concentrations of free analyte. After 30 min, it is clear that the F-nanoMIPs started binding to the MT and after 1 h, dynamic equilibrium was achieved between MIPs bound to MT and free analyte (Figure 4). As it was expected this specific response manifested in increase of fluorescent signal in the presence of higher concentration of specific analyte due to competition between immobilized magnetic template (MT) and free analyte (MP) in solution for binding to F-nanoMIPs.

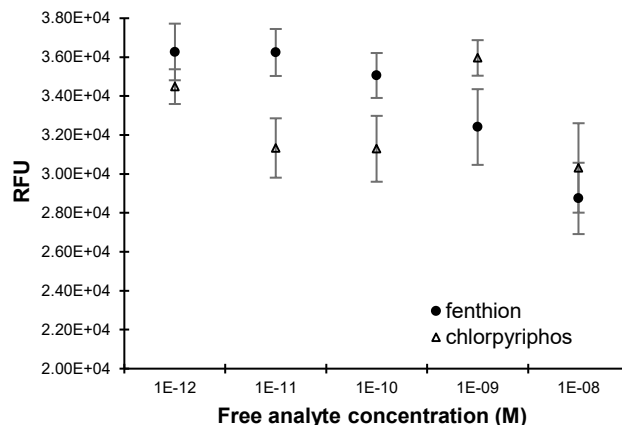


Figure 5. Cross-reactivity in the magnetic assay for fenthion and chlorpyrifos after 60 minutes of incubation.

In the cross-reactivity tests F and CP were added into the wells instead of MP. The results of cross-reactivity study show the opposite response on increase concentration of non-specific analytes Fenthion and Chlorpyrifos (Figure 5), namely, a reduction of the fluorescent signal, potentially due to fluorescence quenching in the presence of higher concentrations of non-specific analytes. It allows drawing a conclusion that F-nanoMIPs recognise specifically MP but not other structurally similar compounds. It is shown that developed MINA is very specific for methyl parathion as no cross-reactivity is detected for both compounds within tested concentration range.

It is important to stress that such high specificity is provided by shape and functionality of the binding site generated by molecular imprinting especially efficient when MIP nanoparticles are prepared using solid phase approach, which allows collecting the particles with highest affinity and specificity towards the template. Accordingly to our previous studies the nanoparticles prepared using solid phase approach are characterized by high affinity and specificity, in many cases superseding those of natural antibodies.²⁶

Competitive binding in real samples: water and milk. The developed MINA was also tested for its ability to detect MP in the real samples. For this evaluation, filtered-tap water and the middle fraction of ultra-centrifuged milk were spiked with different concentrations of MP. Subsequently, each was added into the microtiter plate wells with MT immobilized on the magnetic inserts, followed by the addition of F-nanoMIPs.

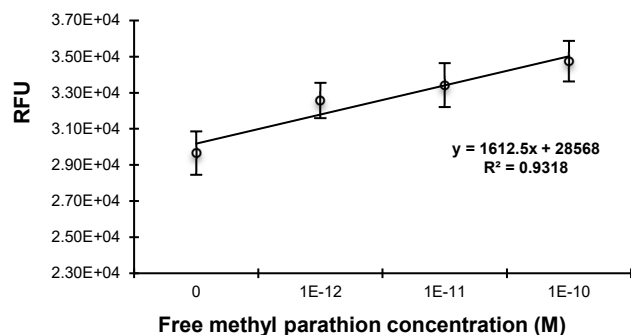


Figure 6. Competitive binding in the magnetic assay for MP after 60 min of incubation in tap water.

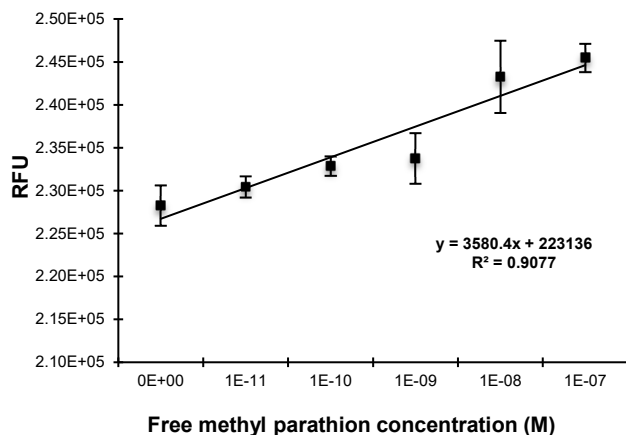


Figure 7. Competitive binding in the magnetic assay for MP after 60 min of incubation in milk.

A linear response in the presence of free analyte MP was clearly observed for both of the real samples. The range was varied depending on the sample type as follows: for the tap water, it was in the range of 1 pM–0.1 nM (Figure 6), whereas for the milk sample, the range was surprisingly wider than in case of blank sample (DI water) as 1 pM–0.1 μ M (Figure 7). Limits of detection were estimated as 5.2 pM and 4.1 pM whereas the limits of quantification were 15.8 pM and 14.9 pM for tap water and milk sample respectively

CONCLUSIONS

We have presented here two types of assays for the detection of MP using nanoMIPs instead of antibodies in pseudo-ELISA format and a completely abiotic MINA where all biological components were substituted by F-nanoMIPs, which functioned as both, specific receptors and reporters, eliminating any need in natural antibodies and enzyme conjugates. Both assays demonstrated an impressive specificity and low sensitivity with LoD in picomolar range and a linearity in the wide concentration range similar to ELISA. In addition, calculated precision and over-all repeatability of used method proved the good quality of the data (Table S1 in SI). It is possible to comment that MINA, with its combination of F-nanoMIPs and the magnetic template, is capable recognising and measuring MP in wider range of concentrations than pseudo-ELISA (pM–nM concentration of MP). The magnetic assay was also proven to work successfully in real samples such as tap water and milk. All

these features are making the performance of the two MIP-based assays comparable with ELISA. Nevertheless, it is important to highlight that both developed assays could be produced at a much lower cost and in a much shorter time scale than ELISA, also benefitting from high stability, long shelf life and no need in cold chain supply essential for antibody and enzyme-based assays.

All protocols developed in this work (e.g. synthesis of nano-MIPs in organics using UV-initiated living polymerization and under aqueous conditions using mechanism of chemical polymerization; immobilization of the template on the magnetic particles; optimization of the polymer composition using molecular modeling and assay optimization and development) can be used for the development of abiotic assays for any analyte of environmental, clinical or biotechnological interest. The produced abiotic MINA uses only low cost, high stability reagents, and requires no washing steps, only the addition of analyte to pre-prepared microtiter plate wells. Furthermore, this assay can be used for the detection of any target molecule, as the imprinting process is not specific for MP. The protocols developed here could potentially be used as a blueprint for the development of abiotic assays for any diagnostic application.

AUTHOR INFORMATION

Corresponding Author

*E-mail: joanna.czulak@mip-dx.com (J. Czulak).

Author Contributions

The manuscript was written through contributions of all authors. All authors have given approval to the final version of the manuscript.

Note

The authors declare no conflict of interest.

ACKNOWLEDGMENT

C. Esen is grateful for the grant from the British Council as the fellow of the Newton Fund Researcher Links Travel Grant (Application ID: 261842976).

The authors would like to thank Francesco Canfarotta from MIP Diagnostics Ltd. for providing the polymerizable fluorescein.

REFERENCES

- (1) Meister, R. 1996. *Methyl parathion*. In *Farm chemicals handbook*, Ed.; Meister R.: Meister Pub Co., Willoughby, Ohio, 1996; *Methyl parathion*.
- (2) Garcia, S.; Abu-Qare, A.; Meeker-O'Connell, W.; Borton, A.; Abou-Donia, M. Methyl Parathion: A Review of Health Effects. *J. Toxicol. Environ. Health B Crit. Rev.* **2003**, *6*, 185–210.
- (3) Liang, H.; Song, D.; Gong, J. Signal-on electrochemiluminescence of biofunctional CdTe quantum dots for biosensing of organophosphate pesticides. *Biosens. Bioelectron.* **2014**, *53*, 363–369.
- (4) Rupa, D. S.; Reddy, P. P.; Reddi, O. S. Cytogeneticity of Quinalphos and Methyl Parathion in Human Peripheral Lymphocytes. *Hum. Exp. Toxicol.* **1990**, *9*, 385–387. ^[1] ^[2] ^[3] ^[4] ^[5] ^[6] ^[7] ^[8] ^[9] ^[10] ^[11] ^[12] ^[13] ^[14] ^[15] ^[16] ^[17] ^[18] ^[19] ^[20] ^[21] ^[22] ^[23] ^[24] ^[25] ^[26] ^[27] ^[28] ^[29] ^[30] ^[31] ^[32] ^[33] ^[34] ^[35] ^[36] ^[37] ^[38] ^[39] ^[40] ^[41] ^[42] ^[43] ^[44] ^[45] ^[46] ^[47] ^[48] ^[49] ^[50] ^[51] ^[52] ^[53] ^[54] ^[55] ^[56] ^[57] ^[58] ^[59] ^[60] ^[61] ^[62] ^[63] ^[64] ^[65] ^[66] ^[67] ^[68] ^[69] ^[70] ^[71] ^[72] ^[73] ^[74] ^[75] ^[76] ^[77] ^[78] ^[79] ^[80] ^[81] ^[82] ^[83] ^[84] ^[85] ^[86] ^[87] ^[88] ^[89] ^[90] ^[91] ^[92] ^[93] ^[94] ^[95] ^[96] ^[97] ^[98] ^[99] ^[100]
- (5) Mathew, G.; Vijayalaxmi, K. K.; Rahiman, M. A. Methyl parathion-induced sperm shape abnormalities in mouse. *Mutat. Res.* **1992**, *280*, 169–173.
- (6) Narayana, K.; Prashanthi, N.; Nayanatara, A.; Kumar, H. H.; Abhilash, K.; Baiyya, K. L. Effects of methyl parathion (o,o-dimethyl o-4-nitrophenyl phosphorothioate) on rat sperm morphology and sperm

count, but not fertility, are associated with decreased ascorbic acid level in the testis. *Mutat. Res.* **2005**, *588*, 28–34. ^[11]

(7) Piña-Guzmán, B.; Solís-Heredia, M. J.; Rojas-García, A. E.; Urióstegui-Acosta, M.; Quintanilla-Vega B. Genetic damage caused by methyl-parathion in mouse spermatozoa is related to oxidative stress. *Toxicol. Appl. Pharmacol.* **2006**, *216*, 216–224. ^[12]

(8) WHO guidelines for drinking water quality “Methyl parathion in drinking water”, 2004, www.who.int/water_sanitation_health/dwq/chemicals/methylparathion.pdf, visited on the 15.11.18.

(9) Public statement for methyl parathion, 2001, www.atsdr.cdc.gov/phs/phs.asp?id=633&tid=117, visited on the 15.11.18.

(10) Mahpishanian, S.; Sereshti, H.; Baghdadi, M. Superparamagnetic core-shells anchored onto graphene oxide grafted with phenylethyl amine as a nano-adsorbent for extraction and enrichment of organophosphorus pesticides from fruit, vegetable and water samples. *J. Chromatogr. A* **2015**, *1406*, 48–58.

(11) Kmešlár, B.; Pareja, L.; Ferrer, C.; Fodor, P.; Fernández-Alba, A. R. Study of the effects of operational parameters on multiresidue pesticide analysis by LC–MS/MS. *Talanta* **2011**, *84*, 262–273.

(12) Machado, I.; Gérez, N.; Pistón, M.; Heinzen, H.; Cesio, M. V. Determination of pesticide residues in globe artichoke leaves and fruits by GC–MS and LC–MS/MS using the same QuEChERS procedure. *Food Chemistry* **2017**, *227*, 227–236.

(13) Ahmadi, K.; Abdollahzadeh, Y.; Asadollahzadeh, M.; Hemmati, A.; Tavakoli, H.; Torkaman, R. Chemometric assisted ultrasound leaching-solid phase extraction followed by dispersive-solidification liquid–liquid microextraction for determination of organophosphorus pesticides in soil samples. *Talanta* **2015**, *137*, 167–173.

(14) Tian, X.; Liu, L.; Li, Y.; Zhou, Z.; Nie, Y.; Wang, Y. Nonenzymatic electrochemical sensor based on CuO–TiO₂ for sensitive and selective detection of methyl parathion pesticide in ground water. *Sens. Actuators B*, **2018**, *256*, 135–142.

(15) Govindasamy, M.; Mani, V.; Chen, S.-M.; Chen, T.-W.; Sundramoorthy, A. K. Methyl parathion detection in vegetables and fruits using silver@graphene nanoribbons nanocomposite modified screen printed electrode. *Sci. Rep.* **2017**, *7*, 46471.

(16) Karthik, R.; Kumar, J.V.; Chen, S.-M.; Kokulnathan, T.; Che, T.-W.; Sakthinathan, S.; Chiu, T.-W.; Muthuraj, V. Development of novel 3D flower-like praseodymium molybdate decorated reduced graphene oxide: An efficient and selective electrocatalyst for the detection of acetylcholinesterase inhibitor methyl parathion. *Sens. Actuators B* **2018**, *270*, 353–361.

(17) Ouyang, H.; Wang, L.; Yang, S.; Wang, W.; Wang, L.; Liu, F.; Fu, Z. Chemiluminescence Reaction Kinetics-Resolved Multianalyte Immunoassay Strategy Using a Bispecific Monoclonal Antibody as the Unique Recognition Reagent. *Anal. Chem.* **2015**, *87*, 2952–2958.

(18) Hua, X.; Yin, W.; Shi, H.; Li, M.; Wang, Y.; Wang, H.; Ye, Y.; Kim, H.J.; Gee, S.J.; Wang, M.; Liu, F.; Hammock, B.D. Development of Phage Immuno-Loop-Mediated Isothermal Amplification Assays for Organophosphorus Pesticides in Agro-products. *Anal. Chem.* **2014**, *86*, 8441–8447.

(19) Wang, P.; Wu, L.; Lu, Z.; Li, Q.; Yin, W.; Ding, F.; Han, H. Gecko-Inspired Nanotentacle Surface-Enhanced Raman Spectroscopy Substrate for Sampling and Reliable Detection of Pesticide Residues in Fruits and Vegetables. *Anal. Chem.* **2017**, *89*, 2424–2431.

(20) Fahimi-Kashani, N.; Rashti, A.; Hormozi-Nezhad, M.; Mahdavi, V. MoS₂ quantum-dots as a label-free fluorescent nanoprobe for the highly selective detection of methyl parathion pesticide. *Anal. Methods* **2017**, *9*, 716–723.

(21) Munawar, H.; Smolinska-Kempisty, K.; Garcia Cruz, A.; Canfarotta, F.; Piletska, E.; Karim, K. and Piletsky, S. A. Molecularly imprinted polymer nanoparticle- based assay (MINA): application for fumonisin B1 determination. *Analyst* **2018**, *143*, 3481–3488.

(22) Tang, S.-P.; Canfarotta, F.; Smolinska-Kempisty, K.; Piletska, E.; Guerreiro, A. and Piletsky S. A pseudo-ELISA based on molecularly

imprinted nanoparticles for detection of gentamicin in real samples. *Anal. Methods* **2017**, *9*, 2853–2858.

(23) Sun, H.; Scharff-Poulsen, A. M.; Gu, H.; Almdal, K. Synthesis and characterization of radiometric, pH sensing nanoparticles with covalently attached fluorescent dyes. *Chem. Mater.* **2006**, *18*, 3381–3384.

(24) Canfarotta, F.; Poma, A.; Guerreiro, A.; Piletsky, S. Solid-phase synthesis of molecularly imprinted nanoparticles. *Nat. Protoc.* **2016**, *11*, 443–455.

(25) Chianella, I.; Guerreiro, A.; Moczeko, E.; Caygill, S.; Piletska, E. V.; Perez De Vargas Sansalvador, I. M.; Whitcombe, M. J.; Piletsky, S. A. Direct replacement of antibodies with molecularly imprinted polymer nanoparticles in ELISA - development of a novel assay for vancomycin. *Anal. Chem.* **2013**, *85*, 8462–8468.

(26) Smolinska-Kempisty, K.; Guerreiro, A.; Canfarotta, F.; Cáceres, C.; Whitcombe, M. J.; Piletsky, S. A comparison of the performance of molecularly imprinted polymer nanoparticles for small molecule targets and antibodies in the ELISA format. *Sci. Rep.* **2016**, *6*, 37638.

(27) Piletska, E. V.; Piletsky, S. S.; Guerreiro, A.; Karim, K.; Whitcombe, M. J.; Piletsky, S. A. Microplates with enhanced immobilization capabilities controlled by a magnetic field. *JCAMS* **2014**, *118*–129.

(28) Piletsky, S. S.; Rabinowicz, S.; Yang, Z.; Zagar, C.; Piletska, E. V.; Guerreiro, A.; Piletsky, S. A. Development of molecularly imprinted polymers specific for blood antigens for application in antibody-free blood typing. *Chem. Comm.* **2017**, *53*, 1793–1796.

(29) Ouyang, H.; Wang, W.; Shu, Q.; Fu, Z. Novel chemiluminescent immunochromatographic assay using a dual-readout signal probe for multiplexed detection of pesticide residues. *Analyst* **2018**, *143*, 2883–2888.

(30) Poma, A.; Guerreiro, A.; Whitcombe, M. J.; Piletska, E. V.; Turner, A. P. F.; Piletsky, S.A. Solid-Phase Synthesis of Molecularly Imprinted Polymer Nanoparticles with a Reusable Template–“Plastic Antibodies” *Adv. Funct. Mater.* **2013**, *23*, 2821–2827. ^[13]

(31) Moczeko, E.; Poma, A.; Guerreiro, A.; de Vargas Sansalvador, I. P.; Caygill, S.; Canfarotta, F.; Whitcombe, M. J.; Piletsky, S. Surface-modified multifunctional MIP nanoparticles *Nanoscale* **2013**, *5*, 3733–3741. ^[14]

(32) Poma, A.; Guerreiro, A.; Caygill, S.; Moczeko E.; Piletsky, S. Automatic reactor for solid-phase synthesis of molecularly imprinted polymeric nanoparticles (MIP NPs) in water. *RSC Adv.* **2014**, *4*, 4203–4206.

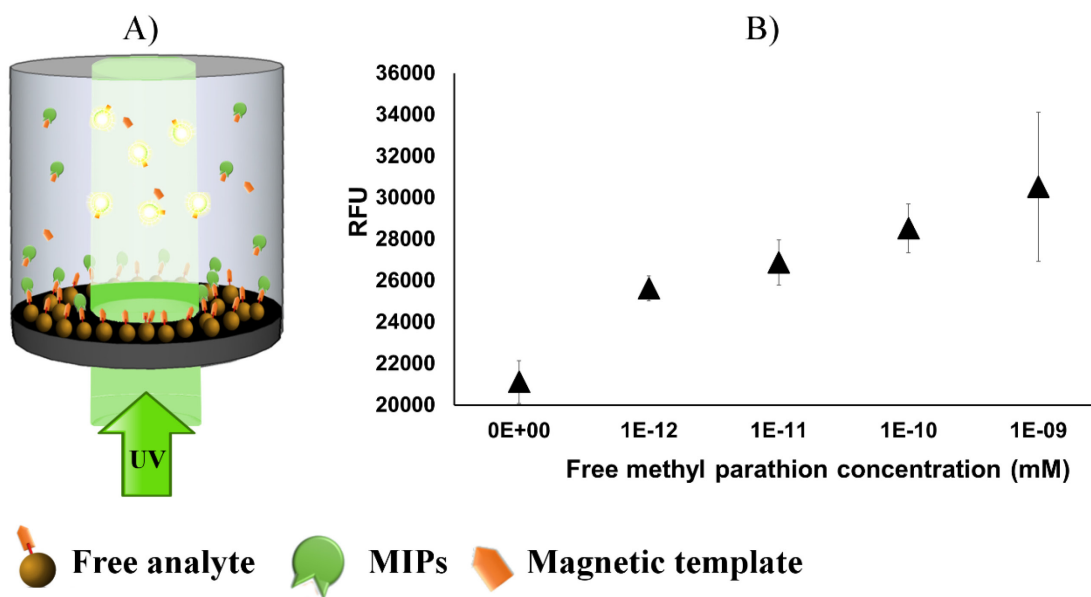
(33) Piletska, E. V.; Guerreiro, A.; Whitcombe, M. J.; Piletsky, S. A. Influence of the Polymerization Conditions on the Performance of Molecularly Imprinted Polymers. *Macromolecules* **2009**, *42*, 4921–4928. ^[15]

(34) Poma, A.; Turner, A. P. F.; Piletsky, S. A. Advances in the manufacture of MIP nanoparticles. *Trends Biotechnol.* **2010**, *28*, 629–637. ^[16]

(35) Turkmen, D.; Bereli, N.; Corman, M. E.; Shaikh, H.; Akgol, S.; Denizli, A. Molecular imprinted magnetic nanoparticles for controlled delivery of mitomycin C. *Artif. Cells, Nanomed., Biotechnol.* **2014**, *42*, 316–322. ^[17]

(36) Cáceres, C.; Canfarotta, F.; Chianella, I.; Pereira, E.; Moczeko, E.; Esen, C.; Guerreiro, A.; Piletska, E.; Whitcombe, M. J.; Piletsky, S. A. Does size matter? Study of performance of pseudo-ELISAs based on molecularly imprinted polymer nanoparticles prepared for analytes of different sizes. *Analyst* **2016**, *141*, 1405–1412.

(37) Basozabal, I.; Guerreiro, A.; Gomez-Caballero, A.; Aranzazu Goicolea M.; Barrio, R. J. Direct potentiometric quantification of histamine using solid-phase imprinted nanoparticles as recognition elements. *Biosens. Bioelectron.* **2014**, *58*, 138–144.



A) Schematic of fluorescent competitive assay in the presence of free analyte and magnetic template,

B) Competitive assay for fluorescent MIPs in the presence of free methyl parathion

Table of Contents artwork here